

GIANT HAWAIIAN LANDSLIDES¹

James G. Moore and William R. Normark

US Geological Survey, Menlo Park, California 94025

Robin T. Holcomb

US Geological Survey, University of Washington, Seattle,
Washington 98195

KEY WORDS: Hawaiian Ridge, slump, debris avalanche

INTRODUCTION

Dozens of major landslides have recently been discovered on the submarine flanks of the Hawaiian Ridge (Figures 1 and 2). These landslides are among the largest on Earth, attaining lengths greater than 200 km and volumes of several thousand cubic kilometers. Two general types of giant landslides, slumps and debris avalanches, are identified, but many intermediate forms occur. These were revealed during a 1986–1991 swath sonar mapping program of the United States Hawaiian Exclusive Economic Zone, a cooperative venture by the U.S. Geological Survey and the British Institute of Oceanographic Sciences. Employed in that work was the long-range side-looking sonar system GLORIA, which records acoustic backscatter from the seafloor in an effective swath 25–30 km wide centered on the survey ship track (Somers et al 1978). The area mapped along the Hawaiian Ridge—2200 km long by 600 km wide—includes about 1.3 million km².

This article reviews general features of the landslides, including criteria for identification, types, relation to volcano structure, mechanism of formation, and degradation with age. Detailed information is presented for a few examples. Discovery of the remarkably common occurrence of giant

¹The US government has the right to retain a nonexclusive, royalty-free license in and to any copyright covering this paper.

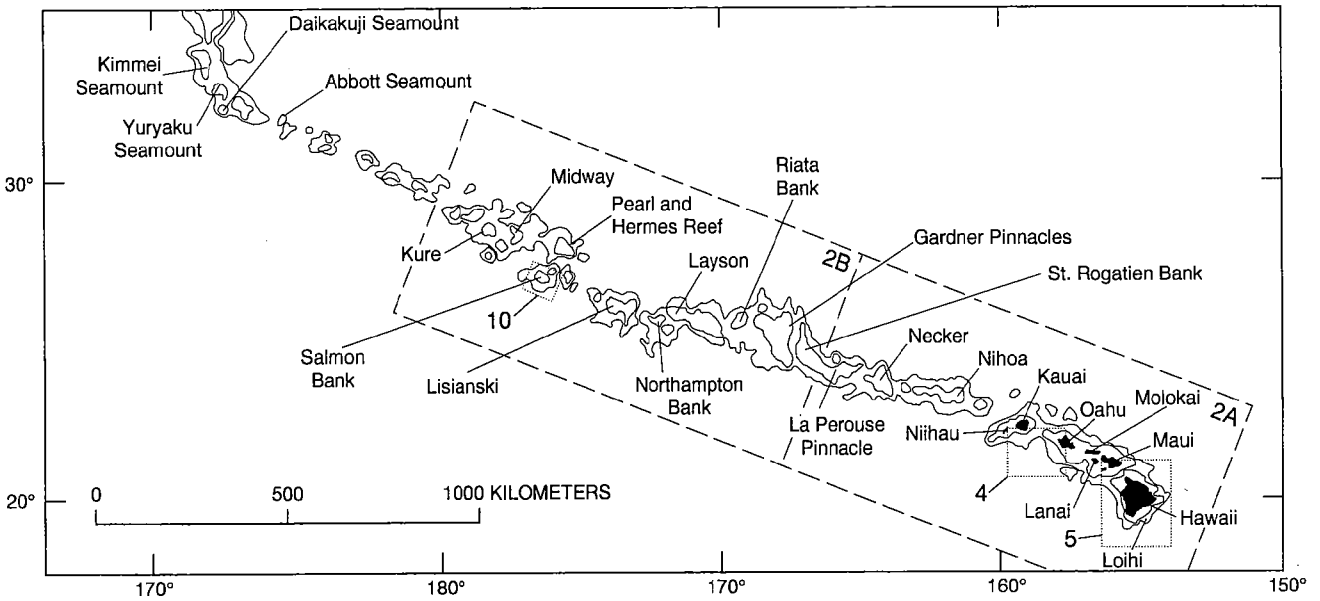


Figure 1 Bathymetry of the Hawaiian volcanic chain with contours at 1 and 2 km depths shown in area of the chain only (after Clague & Dalrymple 1987). Age of volcanoes at the bend, near Kimmei seamount, is about 40 Ma; volcanoes on the island of Hawaii are still active. Dashed boxes indicate areas of Figures 2A, 2B, 4, 5, and 10.

landslides on the Hawaiian Ridge has led to the realization that such forms of mass wasting occur on the submarine flanks of other large marine volcanoes the world over.

GEOLOGIC SETTING OF HAWAIIAN RIDGE

The Hawaiian Ridge was produced by ascent of heat and fluids from a mantle hotspot centered beneath the present island of Hawaii at the southeast end of the ridge. Eruptions of basaltic lava above the hot spot built a succession of giant marine volcanoes. As each volcano grew, movement of the Pacific lithospheric plate toward the west-northwest carried the volcanic edifice away from the hotspot, eventually causing it to become extinct when the feeding conduit was cut. As older volcanoes approached extinction, newer ones grew adjacent to them on oceanic crust newly brought over the hotspot. Long continuation of this process built the present Hawaiian Ridge into a volcanic chain thousands of kilometers long with a few still active volcanoes at its southeast end.

The load of the volcanoes has depressed the underlying lithosphere forming a moat-like depression flanking the ridge—the Hawaiian Trough, and an outer bulge seaward of the moat—the Hawaiian Arch. The axis of the Trough, with sea-floor depths commonly exceeding 5 km, is about 140 km from the ridge axis and is partially filled with volcanoclastic material derived from mass wasting of the adjacent volcanoes. The axis of the broad Arch is about 250 km from the ridge axis and is generally about 4.5 km deep. The morphologic expression of both the Trough and Arch are lost with age primarily as a result of sedimentary infilling of the Trough.

During growth of the Hawaiian Ridge the Pacific plate moved about 9 cm/yr west-northwest. This rate is based on radiometric ages of lava flows erupted near the end of each volcano's shield-building period (Clague & Dalrymple 1987). Hence the volcanoes of the ridge form a continuous age sequence. The volcano of Midway Island grew about 28 million years ago and the volcanoes of Hualalai, Mauna Loa, and Kilauea, of the island of Hawaii 2000 km southeast, grew only during the last few hundred thousand years and are still active. The subaerial form of the volcanoes clearly reflects this age difference. The older northwest volcanoes are deeply incised or eroded to sea level, capped by coral reefs, and deeply submerged. In contrast, the submarine flanks of the volcanoes age slowly and are relatively well-preserved. Age-related differences in volcano morphology of the older volcanoes as compared to the younger and active ones are much less below sea level than above.

Although submarine landsliding occurs throughout the growth of the

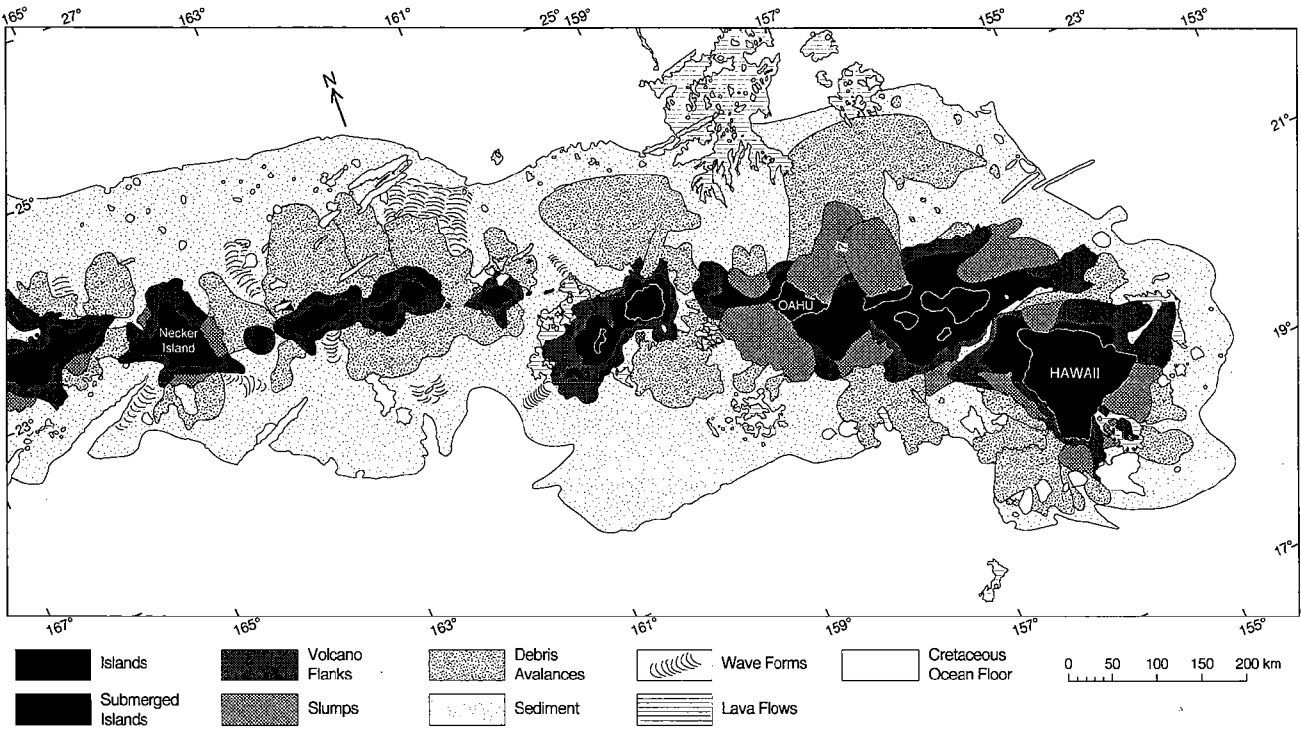


Figure 2A Generalized geologic map of the Hawaiian Ridge. See Figure 1 for location.

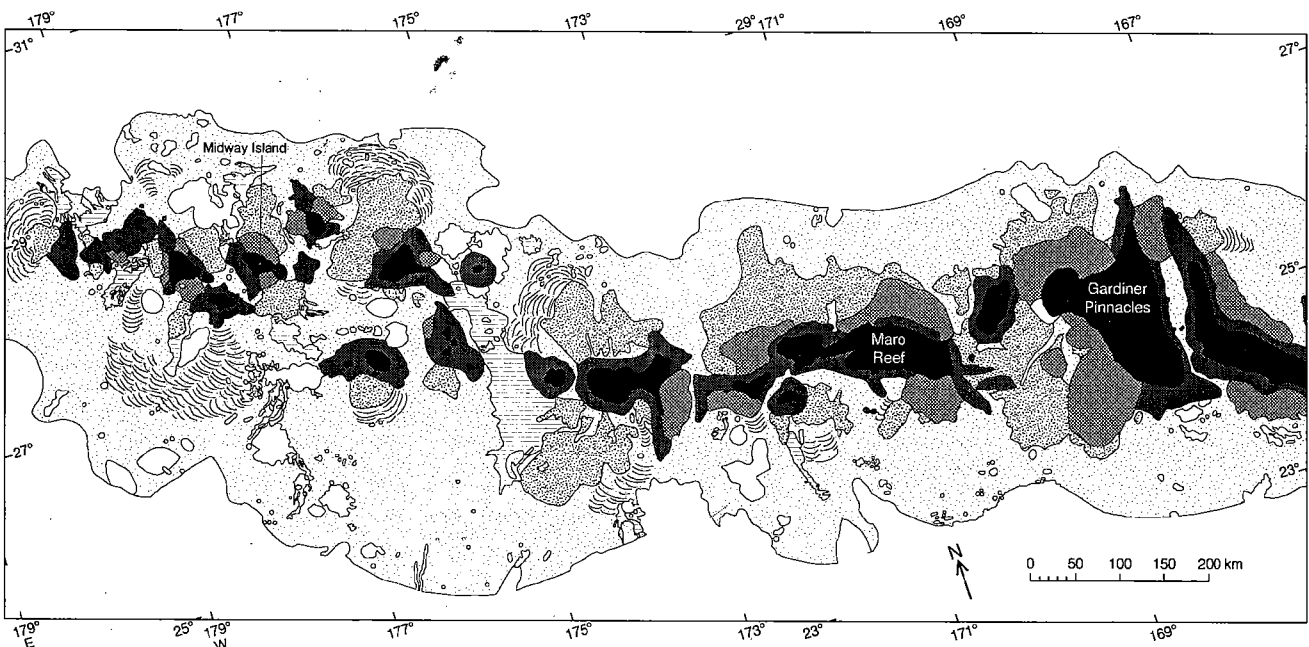


Figure 2B Generalized geologic map of the Hawaiian Ridge. See Figure 1 for location.

volcanoes (and is present on the embryonic Loihi volcano), the largest landslides apparently occur late in the period of active shield growth when the volcanoes are close to their maximum size, are young and unstable, and when seismic activity is high. Hence, the ages of volcanoes along the ridge are mirrored by the ages of their associated landslides.

DISTRIBUTION OF LANDSLIDES

At least 68 major landslides more than 20 km long occur along a 2200 km stretch of the Hawaiian Ridge from 200 km northwest of Midway (180° W longitude) to the island of Hawaii (154° W longitude; Figure 2). Hence the giant landslides average one every 32 km or one every 350 ka. Landslides cover about one half of the flanks of the ridge. Surprisingly the western landslides, which are nearly 30 million years older than the younger ones on the eastern end of the ridge, appear well preserved on sonar side-scan images. The maximum length of landslides apparently increases from 50–100 km at the older west end of the mapped area to 150–300 km at the younger east end (Figure 3*a*). This trend may result in part from thicker post-sliding sediment covering the lower-relief distal parts of older debris fields. A similar relation, however, is apparent for slumps (Figure 3*a*), which have higher relief that is less likely to be obscured by sediment cover; this circumstance suggests that indeed the landslides tend to be longer and larger toward the younger end of the ridge.

Although landslides are equally numerous on the northeast and southwest flanks of the ridge, the larger ones tend to be directed more toward the older (west-northwest) end of the ridge, rather than normal to the ridge (Figure 3*b*). This tendency may result from the greater chance of preservation of landslides toward the trailing, rather than leading, end of the propagating volcanic ridge. All landslides that move approximately east-southeast, for instance, off the actively-growing end of the ridge, become covered by continued growth of the ridge.

In addition to the giant landslides described here that are readily detectable in deep water on small-scale GLORIA images, medium-sized landslides having volumes of tens of km³ are common in shallower water. However, these potentially active landslides of intermediate size have not been adequately mapped because of the difficulties of conducting side-scan sonar surveys in shallow water near the coast. As a result, the hazard of submarine landsliding cannot be estimated well from available data; a better assessment must await detailed studies of smaller but more frequent landslides (Normark et al 1993).

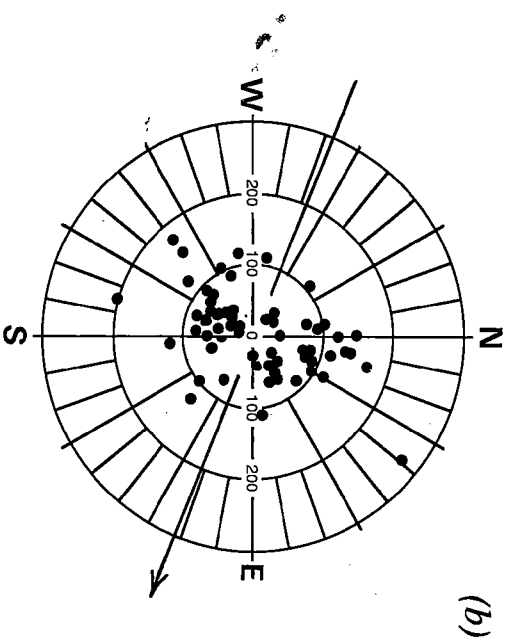
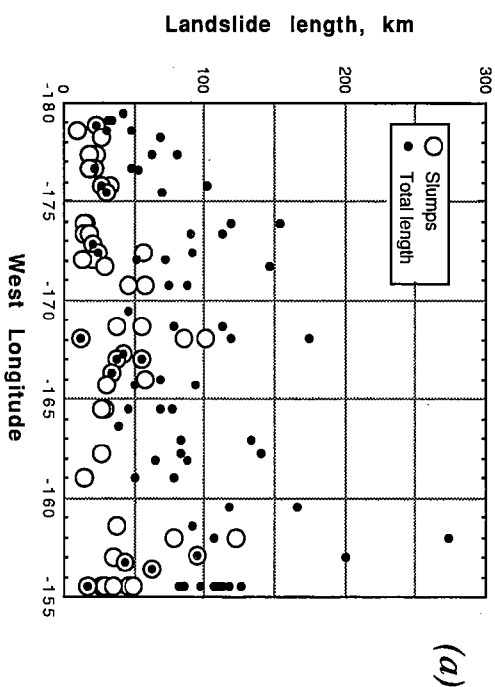


Figure 3 Features of Hawaiian submarine landslides longer than 20 km. (a) Length of slumps and total length of landslides relative to longitude. (b) Direction of slide movement relative to total length of landslide in km. Arrow shows trend of Hawaiian Ridge.

CHARACTER OF LANDSLIDES

The mass wasting features on the Hawaiian Ridge comprise a continuum ranging in size over several orders of magnitude. The general term "landslide" is used herein for all forms of mass movement from incipient slumping that has only slightly disrupted the structural coherence of the volcano flanks, through various degrees of disaggregation, to long-runout avalanches in which fragmentation has totally disrupted and dispersed original volcanic structures. The large landslides described here (more than 20 km long) have been grouped by morphology and degree of dislocation into two major types: slumps and debris avalanches. Because oversteepened parts of slumps may fail as debris avalanches, facies of both types commonly occur in the same landslide. This terminology (after Moore et al 1989) is based on criteria derived from GLORIA sonar images and will no doubt be modified as we learn more about these giant landslides.

Landslide morphology is better preserved below sea level than above because of the lower likelihood of erosion or cover by younger lava. However, many subaerial topographic features owe their origin to landslide processes. All of the major fault systems on the island of Hawaii, as well as subtle changes of slope that probably reflect buried fault scarps, can be related to landslides. The rift zones that radiate from many volcano summits may reflect the primary pull-apart regions at the heads of giant slumps (Moore & Krivoy 1964) or zones of gravitational spreading. Large erosional canyons on several of the islands seem to form within the oversteepened amphitheaters at the heads of giant debris avalanches (Moore et al 1989). The three largest historic earthquakes on the island—those of 1868, 1951, and 1975, all of magnitude 7 or greater—were apparently related to incremental movement of giant slumps (Moore & Mark 1992).

Slumps

Large slumps are deeply rooted in the volcanic edifice and may extend back to the volcanic rift zone and down to the base of the volcanic pile. Slumps may creep over an extended period as they keep pace with the load of volcanic material erupted on their upper part. The slumps are as much as 110 km wide and 10 km thick, and have an overall gradient greater than 3°. In the upper tensional part of the slumps, transverse normal faults marked by scarps commonly bound a few large tilted blocks that may be tens of km in length and several km in width (Figure 4). The compressional regime in the lower part of the slumps is marked by broad bulges, closed depressions, and steep toes. Despite faulting and dislocation, the slumps generally maintain an overall coherent lobate shape by which they are identified in GLORIA images (Figure 4). Parts of the slumps may collapse

and produce a debris avalanche that extends downslope beyond the low end of the slump (Compare Figures 4 and 2). Such compound landslides are common.

The active Hilina slump on the south flank of Kilauea (Figures 5 and 6) may serve as a model of giant slump behavior. However, we know on that the upper few kilometers are the site of repeated dike injection processes and structures below are still a matter of uncertainty. During magnitude 7.2 earthquake in 1975, a 60-km length of Kilauea's south coast subsided as much as 3.5 m and moved seaward as much as 8 m. The Hilina fault system was reactivated over a length of 30 km with normal fault downthrown toward the sea (Tilling et al 1976, Lipman et al 1985). In addition to such episodes of rapid movement, the south flank of the volcano also is creeping seaward continuously as indicated by frequent



Figure 4 GLORIA sonar image (20.5–22°N lat; 158–160°W long) showing contrast between debris avalanche and slump. The south Kauai debris avalanche (with speckled reflector extends 100 km south of the island of Kauai (K) and the Waianai slump (with northwesterly trending scarps) extends 65 km southwest of Oahu (O). Vertical dimension (north-south) image is 167 km. See Figure 1 for location.

repeated geodetic measurements. The east rift zone itself seems to define the pull-apart zone; the region north is stable whereas the region south, extending to the coast and beyond, is moving south at about 6 cm/year (Segall et al 1992).

Drill holes near the axis of the rift zone have penetrated coral reef

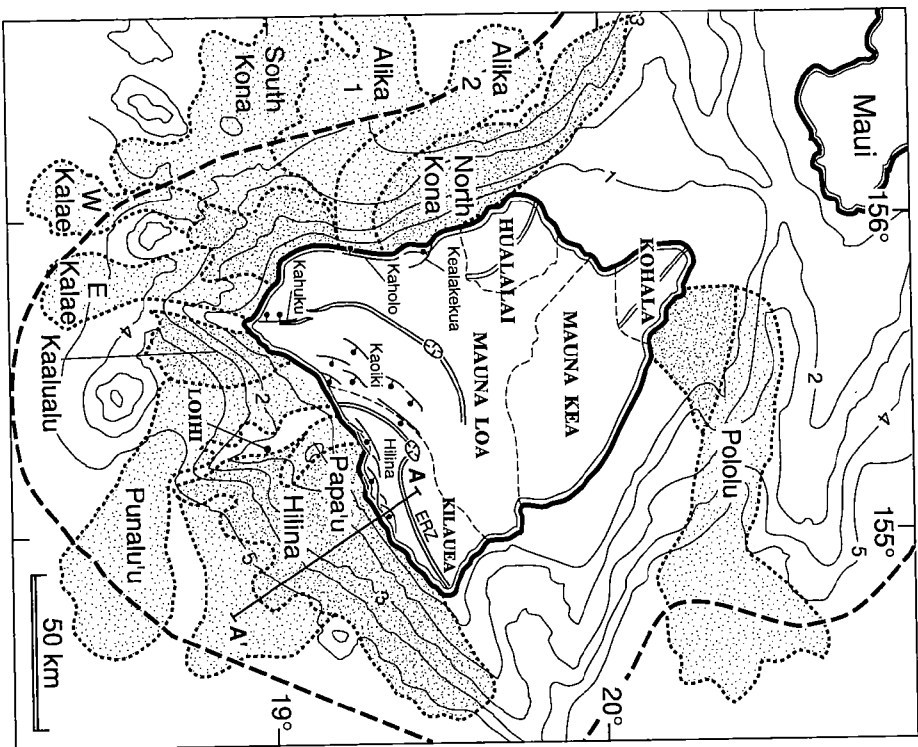


Figure 5 Island of Hawaii and offshore bathymetry; depth contours in kilometers. Dashed lines outline the five volcanoes that compose the island. Dark pattern—major slumps; light pattern—debris avalanches; fine lines—major fault systems (ball on downthrown side); heavy dashed line—axis of Hawaiian Trough; double lines—volcanic rift zones (ERZ, Kilauea's east rift zone). Profile located along line A-A' shown in Figure 6.

deposits more than 1300 m below sea level—deeper than can be attributed to regional subsidence of Kilauea (Thomas 1992). These near-deposits mark a period of stability and lack of neighboring volcanism indicate that dramatic changes have recently occurred in this region.

Most earthquake hypocenters near the east rift zone occur in two group bands that parallel the rift zone at depths of 0–5 and 5–13 km shallower band coincides with the surface trace of vents and cones, rift zone, whereas the deeper band is centered about 4 km seaward, rift zone (Klein et al 1987). The seismic gap 1–3 km wide between bands (as viewed in map plan) is believed to reflect the presence elongate mass or master dike of hot magma (or zone of plasticity) the core of the rift zone (Figure 6). Such a fluid core to the rift zone been postulated earlier because of the need for secondary magma sites to account for the greater volumes of erupted lava as compared the volume of summit subsidence (Swanson et al 1976). The master serves both as the conduit conducting magma from the sub-summit chamber out the rift zone, and as the primary pull-apart zone at the of the Hilina slump permitting spreading of the mobile south flank volcano (Delaney et al 1990, Borga & Treves 1992).

The shallow band of earthquakes above this master dike results brittle fracturing as cracks propagate to the surface to accommodate spreading of the rift zone. These cracks conduct magma upward from master dike in the core of the rift zone through thin feeder dikes to eruvents along the rift zone. Major aseismic decoupling takes place in liquid or plastic core of the master dike. The deeper earthquakes o

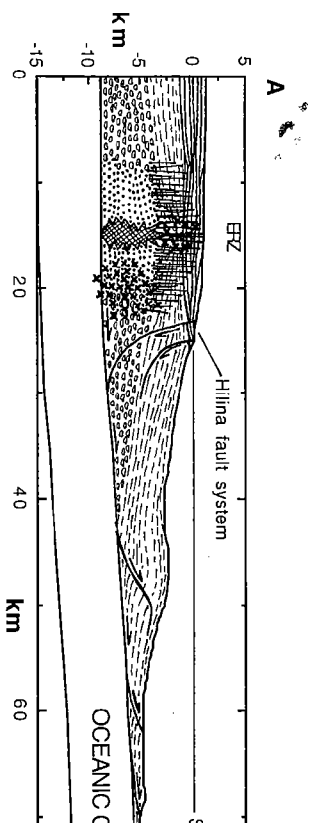


Figure 6 Cross section of the Hilina slump with east rift zone (ERZ) of Kilauea at its no vertical exaggeration. Horizontal layering—subaerial lava; dashed layering—frag lava debris (hyaloclastite); ellipses—pillow lava; vertical lines—sheeted dikes; dotted pattern—gabbro; cross-hatched pattern—magma; crosses—generalized location of earth hypocenters (Klein et al 1987). Modified from Lipman et al 1985, Delaney et al 1990, & Treves 1992. See Figure 5 for location.

seaward side of the master dike result from fracturing and faulting in the south flank as it decouples from the unmoving lower regions and adjusts in zones of stress concentration where the rock is cool enough to fracture.

The slump is bounded below by a major décollement that probably slopes upward from near the base of the volcanic pile at about 10 km below sea level to the ocean floor 5 km deep 50 km seaward. This sliding surface probably coincides in part with the base of the Hawaiian volcanic edifice where it rests on Cretaceous oceanic crust. At its shallower southern part the slump movement is probably facilitated by poorly consolidated, volcanogenic and pelagic sediment on the oceanic crust, and on its deeper, northern part by a hot plastic zone related to magma within the rift zone (Figure 6). The depth extent of the Hilina fault system and whether it connects with the base of the slump is debatable because offshore movement proceeds almost aseismically. These faults may reach to the décollement or curve to join major lithologic discontinuities within the slump (Figure 6).

A steady state movement of the slump by spreading away from the molten core of the rift-zone master dike and solidification of the margins of the master dike will cause the rift zone to migrate seaward at one half the rate of rift-zone opening or slump movement (Hill & Zucca 1987). This spreading will develop a three-fold layering in both the stable or nonsliding part of the volcano and the upper part of the slump, consisting of: a shallow layer of lava flows and hyaloclastites fed from eruptive vents on the rift zone, an intermediate sheeted dike complex of volcanic feeder dikes, and a deep gabbroic layer of solidified walls of the master rift-zone dike (Borgia & Treves 1992).

A major submarine bench about 3000 m deep on the Hilina slump is 35 km long and as wide as 15 km and parallels the subaerial Hilina fault system. This bench is widest downslope from the region where south-flank earthquakes are most concentrated. Elevated ridges near the outer (southern) edge of the bench bound several closed depressions, some of which are more than 100 m deep. The presence of these unfilled, closed depressions below an area where lava flows frequently enter the sea and feed fragmental debris downslope, demonstrates that the bench is tectonically active. The depressions are forming faster than they are being filled.

Growth of the bench is apparently related to a major thrust fault in the lower, compressional part of the Hilina slump (Figure 6). Thrusting elevates the seaward part of the bench and creates a steep scarp 2 km high along the southeast side of the bench. Borgia et al (1990) suggest that such thrusts are probably blind thrusts surmounted by folds.

Three arcuate ridges that are convex southeast occur at the low submarine reaches of the Hilina Slump immediately adjacent to the undisturbed deep sea floor near the axis of the Hawaiian Trough. These ridges are 8 to 13 km long and 500 to 700 m high along their southern flank. They are apparently uplifted by additional thrust faults branching from the primary décollement at the base of the Hilina slump, and probably mark the farthest extension of the slump onto the apron of debris around the foot of the volcano (Figure 6). Hummocks from related debris avalanches extend somewhat farther seaward.

The similarity of the east rift zone of Kilauea, and Hawaiian rift zone in general, to oceanic spreading ridges has been discussed by Holcomb Clague (1983), Hill & Zucca (1987), and Lonsdale (1989). The general model of formation of the massive slumps by spreading from an elongate rift-zone magma chamber at their upper part, and overriding undisturbed seafloor at their lower part, has led Borgia & Treves (1992) to view the Hawaiian volcanoes as a link between volcanic processes and ocean tectonic plates. The spreading volcanic rift zone, where extrusive and intrusive layers are generated, corresponds to the oceanic spreading ridge and the lower part that overrides the ocean floor is "analogous to the overthrusting of a subduction zone accretionary prism" (Thurber & Grip 1988).

Debris Avalanches

The debris avalanches are more surficial features as compared with the giant slumps. They are commonly longer, thinner, and less steep, and have a well-defined amphitheater at their head and hummocky terrain in their lower part. The debris avalanches are 0.05–2 km thick, as much as 230 km long, and possess an overall gradient of less than 3°. Some have apparently formed by catastrophic failure of oversteepened slumps. Rapid movement of avalanches in single events is indicated by their thinness and great length, by movement up the slope of the Hawaiian Arch of their distal reaches in some places (Moore et al 1989), and by their hummocky, fragmented distal regions that closely resemble those of known catastrophic subaerial volcanic landslides, such as those at Mount St. Helens (Voight et al 1981) and Mt. Shasta (Crandell et al 1984).

Amphitheaters commonly are better developed at the heads of the debris avalanches, especially below sea level, than on the slumps. The slow, intermittent nature of slump movement allows the amphitheaters to be filled more completely by the volcanic products erupted during and following movement. The upper part of the East Ka Lae landslide is fed from

a large amphitheater (Moore & Clague 1992), the east wall of which is the subaerial Kahuku fault scarp and its offshore extension (Figure 5). Dikes parallel to the rift zone are exposed along the submarine segment of the scarp indicating that the East Ka Lae debris avalanche cut and steepened the west flank of the submarine rift zone ridge after the southwest rift was established (Moore & Clague 1992).

The upper reaches of the Alika debris avalanches are smooth talus slopes extending from the shoreline down to 2 km depth (Figures 5 and 7). The landslide amphitheaters are not obvious above sea level because they are covered by extensive young lava flows from Mauna Loa. Anomalously steep slopes, however, in a zone 15 km wide extending 8 km inland upslope from the Alika debris avalanches may reflect a landslide amphitheater that is now largely filled and covered by younger lava flows (Moore & Mark 1992). The entire west flank of Mauna Loa is steeper than normal shield slopes and probably results from lava flows filling amphitheaters from the earlier North and South Kona and Alika landslides (Figure 7).

Large submarine canyons offshore from the Hawaiian islands commonly incise the amphitheaters of major debris avalanches, and can be traced into some of the major subaerial canyons of Hawaii. Submarine canyons occur on the upper parts of the north Kauai, northeast Oahu, north Molokai, and northeast Hawaii debris avalanches and extend down 800 to 1300 m below sea level. Subaerial valleys between the Ninole Hills, on the southeast flank of Mauna Loa volcano, have been interpreted as partly buried canyons in the amphitheater of a major southeast-directed landslide (Lipman et al 1990). The submarine canyons were apparently carved subaerially after landsliding and were later submerged by regional subsidence. Subaerial canyon cutting in the basaltic bedrock of the amphitheaters was promoted by the oversteepened, and recently stripped slopes, especially in the amphitheaters formed on the windward (northeast) volcano slopes that receive high rainfall.

The Alika-2 debris avalanche, among the youngest recognized, moved west in its upper reaches, but turned north 60° in its middle course and followed the base of the west slope of the volcano (Figures 5, 7). This change in direction of movement could have resulted from deflection by a debris ridge left by the Alika-1 debris avalanche as well as by the small seamount that separates the Alika-1 and -2 landslide tongues. The middle course of the avalanche has a 40 km long flat-floored channel that is 10 km wide flanked by natural levees. Individual levee segments can be traced as far as 12 km, are more than 1 km wide, and rise from 20 to 100 m above the channel floor (Moore et al 1992). Deep-tow side-scan images show that the levees are discontinuous and are commonly composed of piles of individual blocks and hummocks. Other large levees on GLORIA images

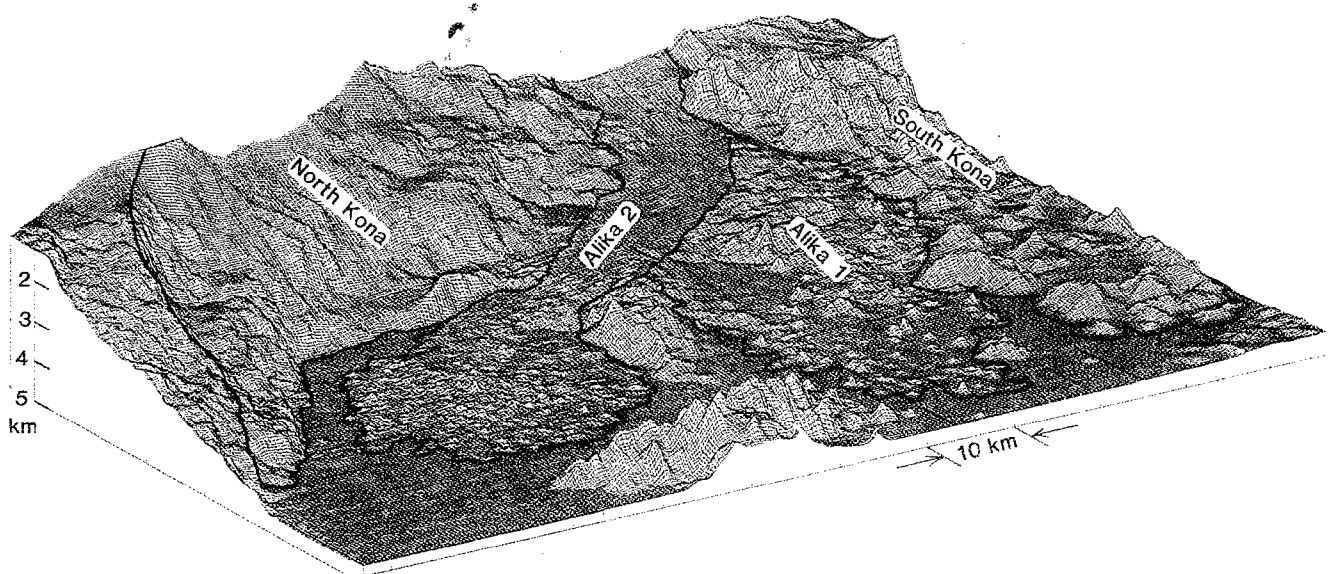


Figure 7 Physiographic view toward the southeast, based on NOAA multibeam bathymetry, of the west submarine flank of Mauna Loa volcano showing four major landslides with 4-fold vertical exaggeration. See area of diagram in Figure 5.

occur in the upper parts of debris avalanches west of Gardner Pinnacles, west of Lisianski, and north of Kauai (Figure 1).

Fields of hummocks or blocky hills are common on the distal parts of debris avalanches. These fields produce a unique speckled pattern on sonar images that is the most defining characteristic of debris avalanches (Figure 4). Multibeam sonar mapping has defined about 190 hummocks from 0.5 to 2 km in size on the 34-km diameter distal lobe of the Alika-2 debris avalanche.

Available data from the Alika landslides suggest that the size distributions of hummocks differ from one avalanche to another. On the Alika-2 avalanche many of the larger hummocks are about 1 km in diameter (Figures 7, 8), whereas on the South Kona avalanche the hummocks are 10 times this size (Figure 7). A full documentation of the range of hummock sizes requires a combination of several scale-dependant techniques (Figure 8). Multibeam echosounding data, gridded at 200 m spacing for production of bathymetric maps, can resolve only those hummocks larger than several hundred meters. Deep-towed side-looking sonar can effectively define blocks from about 5 m to 1 km wide. Photographs by deep-towed cameras can depict blocks and fragments from a few meters to a few centimeters in size. Hundreds of photographs from within the lateral margin of the Alika-2 debris avalanche indicate that smaller fragments occupy the space between the larger blocks and hummocks, and that considerably more than one half the area is littered with fragmental rock material. The volcanic rock fragments are commonly intricately fractured, sharply angular, and show sub-vertical layering that is probably rotated from an original sub-horizontal attitude.

The combined measurements from photographs, deep-towed vehicles, and multibeam bathymetry indicate that a continuum of hummock-block sizes occur from < 1 to 1500 m in size (Figure 8). Widths of blocks or hummocks are several times their height and this factor increases with increasing hummock size so that hummocks exceeding about 1 km in diameter show a diameter:height ratio of about 10:1.

Except for a cover of post-sliding sediment < 0.5 m thick on the Alika-2 debris avalanche, the spacing of the hummocks and blocks is remarkably similar to that of the 1980 Mount St. Helens subaerial volcanic landslide immediately after emplacement. In addition, the diameter-height relations of the hummocks are similar to those of subaerial volcanic debris avalanches such as those of Mount St. Helens (Voight et al 1981) and Mount Shasta (Crandell et al 1984). This similarity further suggests that submarine debris avalanches can move rapidly like the Mount St. Helens avalanche, and therefore pose the secondary hazard of tsunami production (Moore & Moore 1988).

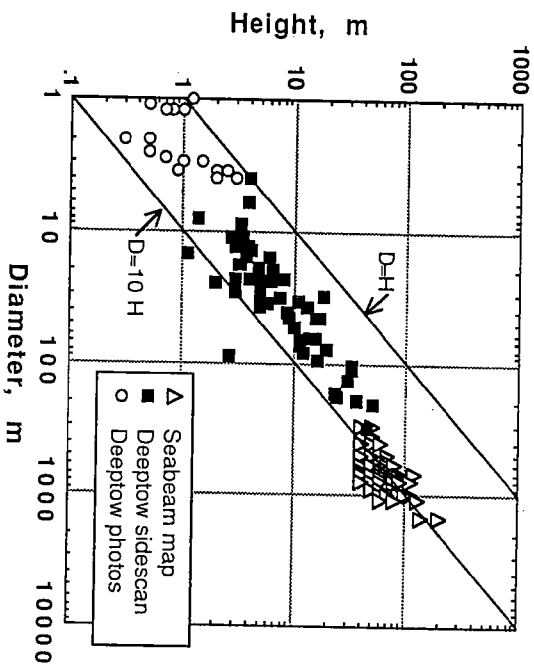


Figure 8 Diameter relative to height of hummocks from distal lobe of Alika-2 slide (see Figure 7 for location). Hummocks range through 3 orders of magnitude in size requiring 3 different methods to image and measure them.

SEDIMENTATION OF LANDSLIDE DEPOSITS

The large debris avalanches provide a major part of the material that fills the Hawaiian Trough. Smaller, and much more frequent, landslides that involve mass wasting of volcanic, coral-reef, and pelagic sediment that accumulates on the flanks of volcanoes provide much of the rest of the fill of the Trough. Along the older part of the Hawaiian Ridge, these mass failures of accumulated sediment are commonly triggered by storm surges and internal waves rather than by earthquakes as is common with the younger volcanoes. The transformation of these smaller landslides to debris flows and turbidity currents effectively distributes the sediment throughout the Trough. The relation of these finer-grained sediment types to the larger debris avalanches and slumps can provide information on the nature and age of landsliding; in turn, the effect of large landslides on the shape of the flanks of the volcanoes can provide long-term controls on the source and transport pathways for the finer-grained sediment.

A seismic reflection survey from Kauai to Hawaii indicates that the northern Trough is filled with as much as 2 km of material deposited in four sequential stages (Rees et al 1993). From the bottom up these stages

are represented by 1. a basal pelagic layer, 2. a layer of volcanoclastic sediments, 3. a layer of landslide debris, and 4. a final layer of turbidite and pelagic sediment. The basal unit of pelagic sediment 50–100 m thick was deposited on the 80-Ma oceanic crust prior to flexural depression. This slowly-deposited sediment comes from a variety of sources including wind blown material, slowly settling fine-grained sediment, and biogenic debris. Layer 2 is bedded sediment that fills the Trough as it begins to rapidly subside due to loading by adjacent downstream volcanoes; much of this transport is by turbidity currents flowing along and across the axis of the moat transporting sediment from erosion and mass wasting of older islands in the chain. The third layer, which locally constitutes the bulk of the fill, includes massive volumes of fragmental volcanic rock that represent an average of four major debris avalanche units, each up to 700 m thick. The top layer of ponded sediment in the deepest part of the trough was apparently largely deposited by turbidity currents after volcanism and subsidence effectively ceased.

Pelagic Sedimentation

The Cretaceous crust as well as the volcanic ridge built upon it in the Hawaiian region is subject to slow and continual pelagic sedimentation. The rate of accumulation of this sediment layer varies from place to place and through geologic time partly because of changes in the amount of fine-grained sediment derived from the growing volcanic ridge. Airborne volcanic ash and wind-blown dust, fine-grained material stirred up by submarine landslides, and material eroded from volcanoes and fringing coral reefs all contribute. An understanding of the general rate of accumulation of pelagic sediment can provide information on the age of the giant landslides.

The sedimentation rate on the Hawaiian Trough and Arch can be determined from sediment thicknesses on the large North Arch lava flow (North of Oahu, Figure 2), which has been dated by magnetostratigraphy of sediment cores and the thickness of the alteration layer (palagonite) formed on the surface of basalt glass exposed to seawater (Clague et al 1990). The rate of sediment accumulation on the lava varies both with age and with distance from the islands. At a distance of about 140 km from the islands, somewhat beyond the axis of the Trough, the rate is 5.8 m/my for the period 1.7 to 1 Ma, and 1.8 m/my for the period 1 to 0.7 Ma. At a distance of about 180 km from the islands, near the axis of the Hawaiian Arch, the rates are less than half those determined near the Trough.

These rates can be compared to those at the Ocean Drilling Program Site 842, 320 km west of the island of Hawaii on the Arch. Since 3.5 Ma an average rate of 3.8 m/my, with variations between 2.5 and 11.6 m/my,

was determined by relating remnant magnetization of the core to the magnetic polarity time scale (Shipboard Scientific Party 1992). Some of the volcanic silt beds at this site, however, have been interpreted as turbidity current deposits generated by the large debris avalanches from Mauna Loa (Garcia et al 1992); turbidite deposition could account for the short periods of higher sedimentation rate.

A third method of estimating pelagic sedimentation rates is by measuring sediment thickness on debris avalanches assuming that the landslide ages approximate the ages of the end of shield-building of their host volcano as determined by K-Ar dating of lava flows (Clague & Dalrymple 1987). The thickness of sediment on the tops of hummocks, where turbidity flow sedimentation is minimized, were measured on 3.5 kHz echo-sounding records for a number of debris avalanches along the ridge. Sediment thickness systematically increases toward the older end of the ridge and the rate approximates 2.5 m/my (Figure 9), which is in general agreement with other estimates described above.

The approximate mean sedimentation rate of 2.5 m/my can be employed to estimate the relative and absolute ages of some of the landslides where sediment thickness can be measured on the tops of hummocks provided that other forms of sediment transport, such as turbidity flows, are not important. The Aikua-2 debris avalanche (Figure 5) is one of the youngest

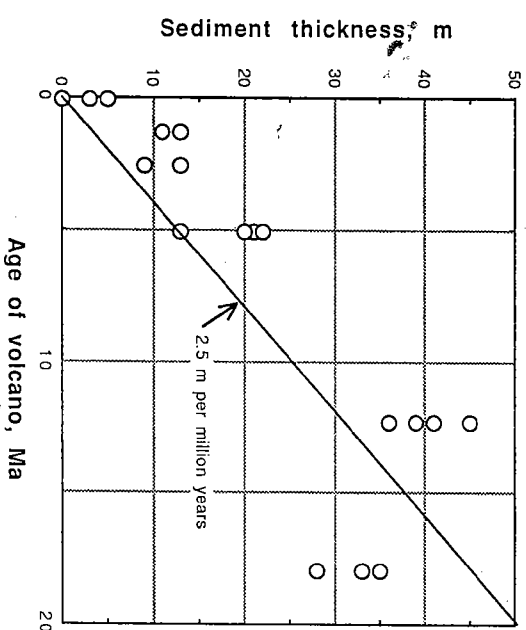


Figure 9 Sediment thickness on top of hummocks of selected landslides as determined from 3.5 kHz echo-sounding records.

for which sediment thicknesses are available. Hundreds of seafloor photographs in the distal hummocky debris field show a sediment cover of only a few tens of centimeters (Moore et al 1992), indicating a maximum age of several 100 ka. Both the Clark and Nuanu debris avalanches, which are southwest of Lanai and northeast of Oahu respectively (Figures 1 and 2), carry about 9 m of sediment atop distal hummocks suggesting that both are about the same age, roughly 3.6 Ma.

Turbidites

Turbidity currents, which generally flow downslope on the flanks of the ridge, are responsible for transporting large volumes of fine sediment locally over great distances. Geophysical evidence indicates that a large proportion of sediment in the Hawaiian Trough 100 km from the ridge axis consists of turbidites (Normark & Shor 1968). Core from an ODP hole on the Hawaiian Arch 320 km west of Hawaii contains turbidite layers containing glass fragments of a composition similar to that of Mauna Loa volcano on Hawaii (Garcia et al 1992); this suggests long distance transport and upslope flow.

Partly covering and extending downslope from several of the landslides are lobate areas that include a few to dozens of large lobate and crescent-shaped wave forms that resemble sediment waves or dunes in GLORIA images (Figure 10). We prefer the term *mud waves*, following the usage of Flood & Shor (1988), because the reflector character on 3.5-kHz reflection profiles is typical of fine-grained sediment. Flood & Shor (1988) also noted that the term "sediment waves" can be correctly used in describing most sinusoidal sediment topography which can include areas of submarine slumps or even basement-controlled topographic relief (e.g. see Dadsman et al 1992). More than two dozen areas of mud waves have been mapped that are 5–75 km in length, and as much as 100 km in width (Figure 2).

The long axes of the mud waves are generally parallel with, and on the downslope extension of, the toe of landslides (Figure 2). The wave fields occur as a distal areole on the lower part of debris avalanches so that the axes of the waves are perpendicular to the movement direction of the adjacent avalanche or are parallel to regional depth contours. The mud waves are common in 4.5 to 5.2 km depth. Wavelengths range from 1.5 to 3.5 km with amplitudes (as measured on 3.5-kHz echosounding records) of 10–30 m. These dimensions are typical of mud waves previously described from a variety of deep-sea depositional environments (Normark et al 1980, Flood & Shor 1988). Although individual wave forms can commonly be traced for 4–10 km, smaller ones that are not well depicted on GLORIA images probably occur. The wavelength-to-amplitude ratio of the wave forms is about 100 to 1 suggesting that their distinctive



Figure 10 GLORIA sonar images of mud waves with wavelength of about 2.5 km on debris avalanche on south flank of Salmon Bank. East-west lines are ship tracks that are about 3 km apart. See Figure 1 for location.

appearance in the GLORIA imagery results from variation in acoustic backscatter of sediment types from the troughs to the crests of the dunes; and not to bathymetric relief.

Prominent chutes, which appear to conduct sediment downslope from now submerged islands and reefs, occur upslope from the wave forms and may be the principal feeding channels for the sediment of the mud waves. Mud waves are more abundant along the western segment of the ridge (Figure 2) and do not appear east of the island of Kauai (160° W long). Restriction of the mud waves to the older part of the ridge suggests that they form slowly by ongoing processes (Flood 1988) after sufficient

sediment has accumulated to cover earlier local relief. Because most of the mud waves occur downslope from now submerged islands that were deeply eroded and thickly capped by coral reefs, it is likely that nearshore processes and pelagic sediment deposition on the upper flanks of the volcanoes contributed the abundant sediment necessary to construct the wave forms. This debris was perhaps added incrementally by downward moving turbidity currents that must have swept over broad areas in order to have deposited and shaped the sediment producing the large coherent fields of mud waves.

Coral Reefs

Waning of volcanic activity at the end of shield building causes relatively passive shoreline conditions that favor the growth and preservation of coral reefs. The rapid subsidence of the volcanoes, resulting from the load they impose on the lithosphere, drown the reefs as much as several km below sea level. Recognition of coral reefs in GLORIA sidescan images has permitted the mapping of the former shorelines of now partly or totally submerged islands (Figure 2).

Commonly, reefs post-date landslides because they grow and are preserved only after the end of vigorous volcanic activity, which appears also to be the primary period of landslide movement. However, continued investigations will no doubt reveal places where landslides have disrupted coral reefs. In the cases examined, the reefs lie on top of the upper part of landslides and therefore the age of the reef will provide a minimum age for landslide movement. For example, an unbroken — 150 m submerged reef at the head of the northern Alike landslide complex and the North Kona landslide has been dated at 18 ka (Moore & Clague 1992) and hence indicates that the Kealakekua fault at the head of these landslides (Figure 5) and subordinate breakaway scarps have been inactive since that time despite minor historic ground cracking (Lipman et al 1988).

LANDSLIDES ON OTHER MARINE VOLCANOES

Large-scale landsliding of marine volcanoes is not restricted to the Hawaiian Ridge. Many examples have been recently discovered at other locations, stimulated in part by the Hawaiian discoveries. Multibeam bathymetric surveys off the island of La Reunion have supported the previously proposed notion that the east side of the active Piton de la Fournaise volcano has failed by massive landsliding (Lenat et al 1989). Many features of Mount Etna, both above and below sea level, have recently been explained by gravitational spreading (Borgia et al 1992). Multibeam bathymetric

maps from the northwestern Pacific reveal evidence for numerous scale landslides on the Emperor and Michelson Ridges as well as seamounts of the Mapmakers and the Marcus-Wake groups (Sm King 1992). Limited multibeam surveys of the southern Galapagos form reveal morphologic similarities with major Hawaiian slumps (Cwick et al 1992).

Re-examination of early GLORIA images has revealed large land on the submarine slopes of the Canary Islands and Tristan de Cunha had previously gone unrecognized (Holcomb & Searle 1991). Petro morphology of the subaerial Marquesas volcanoes coupled with bathymetric surveys has led Barszczus et al (1992) and Filmer et al (1992) to propose major collapse of eight of the volcanoes.

In addition to these recent discoveries, giant landslides on many island volcanoes have long been suspected from topographic anomalies both above and below sea level (Fairbridge 1950). Island asymmetry including broad embayments and high coastal cliffs, commonly oriented seaward side, hint at major submarine landslides. A general survey of oceanic volcanoes led Holcomb & Searle (1991) to conclude that single landslides have removed 10–20% of their source volcanoes, that larger fractions have been removed from a single edifice by multiple landslides. Large landslides have affected oceanic volcanoes ranging in size, geologic setting, and climatic environment.

SUMMARY

Sixty-eight landslides more than 20 km long are present along a 2200 km segment of the Hawaiian Ridge from near Midway to Hawaii. Some of the landslides exceed 200 km in length and 5000 km³ in volume, rank them among the largest on Earth. Most of these giant landslides were discovered during a mapping program of the U. S. Hawaiian Economic Zone from 1986 to 1991 utilizing the GLORIA side-scan sonar mapping system.

Two general types of landslides are present: slumps and debris avalanches. Many intermediate forms occur and some debris avalanche form from oversteepened slumps. The slumps are deeply rooted in volcanoes and may extend back to volcanic rift zones and down to base of the volcanic pile at about 10 km depth. Tension at the upper part is accommodated by major normal faults as well as by pull-apart structures of the volcanic rift zones, and the lower compressional regime is marked by broad bulges, closed depressions, and steep toes. Incremental movement of a few meters on historic slumps has produced major earthquakes (in

nitude > 7). Magma or associated hot zones of plasticity probably enhance basal movement of the upper part, and unconsolidated sediment promotes movement of the lower part. Debris avalanches are thinner, longer, and move on lower gradients than slumps. Their rapid movement is indicated by the fact that some have moved uphill for tens of kilometers, and are believed to have produced major tsunamis. The debris avalanches left large amphitheatres at their heads and produce broad hummocky distal lobes at their toes. Commonly, major canyons have incised the amphitheatres.

Giant landslides have recently been discovered on many other marine volcanoes where they also can be related to volcanic structure and eruptive activity. It is now clear that large-scale collapses of the flanks of oceanic volcanoes are as important as the basic volcanic processes in determining the growth history and final form of the volcanoes. Future studies need to obtain details of the morphology of the landslide deposits and the nature of the transported material to learn about the landslide mechanisms and the interaction of landsliding to the volcanic processes of the host volcano. Detailed multibeam bathymetry and extensive sampling is needed not only for the large debris avalanches but also for the smaller, nearshore landslides that probably occur with more frequency and, therefore, pose a more immediate hazard than the larger failures. Such detailed studies should focus on young and currently active landslides on volcanic islands, such as the Hilina slump on the south flank of Kilauea volcano of Hawaii, where subaerial monitoring of landslide movement, volcanic activity, and seismicity can provide critical clues to the processes involved that are difficult to obtain in deep-marine settings.

ACKNOWLEDGMENTS

This work is largely based on the 1986–1991 swath sonar mapping program of the United States Hawaiian Exclusive Economic Zone, a cooperative venture of the U. S. Geological Survey and the British Institute of Oceanographic Sciences. We are indebted to the crews and technical staffs of the M/V *FARNELLA* for their labors during this work and have benefited from discussions with our colleagues associated with the program. We thank Ellen Lougee who drafted Figures 1, 2, and 5, Carolyn Degnan who prepared Figure 7 from NOAA digital data, and Paul Delaney and David Scholl who critically reviewed the manuscript and provided helpful comments.

Literature Cited

- Barcousz HG, Filmer PE, Desonnie D. 1992. Cataclysmic collapses and mass wasting processes in the Marquesas. *Eos, Trans. Am. Geophys. Union* 73: 313 (Abstr.)
- Borgia A, Burr J, Montero W, Morales LD, Alvarado GE. 1990. Fault propagation folds induced by gravitational failure and slumping of the Central Costa Rica Volcanic Range: implications for large terrestrial and Martian volcanic edifices. *J. Geophys. Res.* 95: 14,357–82
- Borgia A, Ferrari L, Pasquare G. 1992. Importance of gravitational spreading in the tectonic and volcanic evolution of Mount Etna. *Nature* 357: 231–35
- Borgia A, Treves B. 1992. Volcanic plates overriding the oceanic crust: structure and dynamics of Hawaiian volcanoes. *Geol. Soc. London Spec. Publ.* 60: 277–99
- Chadwick WW Jr, Moore JG, Fox CG, Christie DM. 1992. Morphologic similarities of submarine slope failures: south flank of Kilauea, Hawaii, and the southern Galapagos platform. *Eos, Trans. Am. Geophys. Union* 73: 507 (Abstr.)
- Clague DA, Dalrymple GB. 1987. The Hawaiian–Emperor volcanic chain, Part I. *US Geol. Surv. Prof. Pap.* 1350: 5–54
- Clague DA, Holcomb RT, Sinton JM, Detrick RS, Torressan ME. 1990. Pliocene and Pleistocene alkalic flood basalts on the seafloor north of the Hawaiian Islands. *Earth Planet. Sci. Lett.* 98: 175–91
- Crandell DR, Miller CD, Glicken HX, Christensen RL, Newhall CG. 1984. Catastrophic debris avalanche from ancestral Mount Shasta volcano, California. *Geology* 12: 143–46
- Dadisman SV, Marlow MS, Rothwell RG, Harris M. 1992. Cruise report: GLORIA survey of the Hawaiian Island Chain, F2-90-HW. *US Geol. Surv. Open-File Rep.* 92-206, 65 pp.
- Delaney PT. 1992. Motion of Kilauea volcano during sustained eruption from the Puu Oo and Kupāānaha vents 1983–1991. *Eos, Trans. Am. Geophys. Union* 73: 506 (Abstr.)
- Delaney PT, Fiske RS, Miklius A, Okamura AT, Sako MK. 1990. Deep magma body beneath the summit and rift zones of Kilauea volcano, Hawaii. *Science* 247: 1311–16
- Fairbridge RW. 1950. Landslide patterns on oceanic volcanoes and atolls. *Geophys. J.* 115: 84–88
- Filmer PE, McNutt MK, Webb H, Dixon DJ. 1992. Volcanism and archipelagic aprons: a comparison of the Marquesan and Hawaiian islands. *Eos, Trans. Am. Geophys. Union* 73: 313 (Abstr.)
- Flood RD. 1988. A lee wave model for deep-sea mudwave activity. *Deep-Sea Res.* 3: 973–83
- Flood RD, Shor AN. 1988. Mud waves in the Argentine Basin and their relationship to regional bottom circulation patterns. *Deep-Sea Res.* 35: 943–71
- Garcia MO. Scientific Party ODP Leg 134 1992. Volcanic sands from ODP site 84; 300 km west of Hawaii: turbidites from giant debris flows. *Eos, Trans. Am. Geophys. Union* 73: 513–14 (Abstr.)
- Hill DP, Zucca JJ. 1987. Geophysical constraints on the structure of Kilauea and Mauna Loa volcanoes and some implications for seismomagnetic processes. *U. S. Geol. Surv. Prof. Pap.* 1350: 903–17
- Holcomb RT, Clague DA. 1983. Volcanic eruption patterns along submarine rift zones. *Proc. Oceans '83 Conf.* 2: 787–90
- San Francisco: IEEE/MTS
- Holcomb RT, Seatie RC. 1991. Large land slides from oceanic volcanoes. *Mar Geotechnol.* 10: 19–32
- Klein FW, Koyanagi RY, Nakata JS, Tanigawa WR. 1987. The seismicity of Kilauea's magma system. Part II. *US Geol. Surv. Prof. Pap.* 1350: 1019–185
- Lerat J-F, Vincent P, Bachelety P. 1989. The off-shore continuation of an active basaltic volcano: Pion de la Fournaise (Reunion Island, Indian Ocean). *J. Volcanol. Geotherm. Res.* 36: 1–36
- Lipman PW, Lockwood JP, Okamura RT, Swanson DA, Yamashita KM. 1985. Ground deformation associated with the 1975 magnitude-7.2 earthquake and resulting changes in activity of Kilauea volcano, Hawaii. *US Geol. Surv. Prof. Pap.* 1276: 45 pp.
- Lipman PW, Normark WR, Moore JG, Wilson JB, Guimacher CE. 1988. The giant submarine Aikā debris slide, Mauna Loa, Hawaii. *J. Geophys. Res.* 93: 4279–99
- Lipman PW, Rhoads JM, Dalrymple GB. 1990. The Ninole Basalt—implications for the structural evolution of Mauna Loa volcano, Hawaii. *Bull. Volcanol.* 53: 1–19
- Lonsdale P. 1989. A geomorphological reconnaissance of the submarine part of the east rift zone of Kilauea volcano, Hawaii. *Bull. Volcanol.* 51: 123–44
- Moore GW, Moore JG. 1988. Large-scale bedforms in boulder gravel produced by giant waves in Hawaii. *Geol. Soc. Am. Spec. Pap.* 229: 101–10
- Moore JG, Clague DA. 1992. Volcanic growth and evolution of the island of Hawaii. *Bull. Geol. Soc. Am.* 104: 1471–84
- Moore JG, Clague DA, Holcomb RT, Lipman PW, Normark WR, Torressan ME. 1989. Prodigious submarine landslides on

- the Hawaiian Ridge. *J. Geophys. Res.* 94: 17,465-84
- Moore JG, Krivoy H. 1964. The 1962 flank eruption of Kilauea Volcano and structure of the east rift zone. *J. Geophys. Res.* 69: 2033-45
- Moore JG, Mark RK. 1992. Morphology of the island of Hawaii. *GS4 Today* 2: 257-59
- Moore JG, Normark WR, Gutmacher CE. 1992. Major landslides on the submarine flanks of Mauna Loa volcano, Hawaii. *Landslide News* 6: 13-15
- Normark WR, Hess GR, Stow DAV, Bowen AJ. 1980. Sediment waves on the Monterey Fan levees: a preliminary physical interpretation. *Mar. Geol.* 37: 1-18
- Normark WR, Moore JG, Torressan ME. 1993. Giant volcano-related landslides and the development of the Hawaiian Islands. In *Submarine Landslides: Selected Studies in the US Exclusive Economic Zone*, ed. WCS Schwab HILee DCTwicheil. *US Geol. Surv. Bull.* 2002: 184-96
- Normark WR, Shor GG Jr. 1968. Seismic reflection study of the shallow structure of the Hawaiian Arch. *J. Geophys. Res.* 73: 6991-98
- Rees BA, Detrick RS, Coakley BJ. 1993. Seismic stratigraphy of the Hawaiian flexural moat. *Geol. Soc. Am. Bull.* 105: 189-205
- Segall P, Delaney P, Amadottit T, Freymanneller J, Owen S. 1992. Deformation of the south flank of Kilauea Volcano. *Eos, Trans. Am. Geophys. Union* 73: 505-6 (Abstr.)
- Shipboard Scientific Party. Site 842. 1992. In *Proc. Ocean Drilling Prog. Initial Rep.*, ed. A Dziewonski, R Wilkens, J Firth, et al. 136: 37-63. College Station, TX: Ocean Drilling Prog.
- Somers ML, Carson RM, Revie JA, Edge RH, Barrow VJ, Andrews, AG. 1978. GLORIA II—An improved long range sidescan sonar. *Proc. IEEE/ERE Subconf. on Ocean Instr. and Commun., Oceanol. Int.*, pp. 16-24. London: BPS
- Smoot NC, King RE. 1992. Three-dimensional secondary surface geomorphology of submarine landslides on northwest Pacific plate guyots. *Geomorphology* 6: 151-74
- Stearns HT, Macdonald GA. 1946. Geology and ground-water resources of the island of Hawaii. *Hawaii Div. Hydrogr. Bull.* 9: 363 pp.
- Swanson DA, Jackson DB, Koyanagi RY, Wright TL. 1976. The February 1969 east rift eruption of Kilauea Volcano, Hawaii. *US Geol. Surv. Prof. Pap.* 891: 30 pp.
- Thomas DM. 1992. Thermal and structural conditions within the Kilauea east rift zone as indicated by deep drilling data. *Eos, Trans. Am. Geophys. Union* 73: 513 (Abstr.)
- Thurber CH, Gripp AE. 1988. Flexure and seismicity beneath the south flank of Kilauea volcano and tectonic implications. *J. Geophys. Res.* 93: 4271-78
- Tilling RI, Koyanagi RY, Lipman PW, Lockwood JP, Moore JG, Swanson DA. 1976. Earthquakes and related catastrophic events. Island of Hawaii, November 29, 1975. A preliminary report. *US Geol. Surv. Circ.* 740: 33 pp.
- Voight B, Glicken H, Janda RJ, Douglass PM. 1981. Catastrophic rockslide avalanche of May 18. In *The 1980 eruptions of Mount St. Helens, Washington*, ed. PW Lipman, DR Mullineaux. *US Geol. Surv. Prof. Pap.* 1250: 347-400

THE LATE EOCENE-OLIGOCENE EXTINCTIONS

Donald R. Prothero

Department of Geology, Occidental College, Los Angeles, California 90041

KEY WORDS: Antarctic, glaciation, fossil mammals, foraminifera, climate change

INTRODUCTION

The transition from the Eocene to the Oligocene Epochs, from about 40 to 30 Ma (million years ago), was the most significant interval in Earth history since the dinosaurs died out 65 Ma. From the warm, equable "greenhouse" climate of the early Eocene (a relict of the age of dinosaurs), the Earth experienced major climatic changes: Global temperature plummeted, and the first Antarctic ice sheets appeared. These climatic stresses triggered extinctions in plants and animals, both on land and in the oceans. By the early Oligocene (33 Ma), the Earth had a much cooler, more temperate climate, with a much lower diversity of organisms. Indeed, the Eocene-Oligocene transition marked the change from the global "greenhouse" world of the Cretaceous and early Cenozoic to the glaciated "ice house" world of today.

Despite the intense research interest in mass extinctions over the past two decades, the Eocene-Oligocene extinctions have been relatively understudied and misunderstood. While hundreds of papers have been published on the terminal Cretaceous extinction of dinosaurs and ammonites since the discovery of the iridium anomaly in 1980, only a few dozen articles have been published on the Eocene-Oligocene extinctions. Much of this work has now been invalidated by new data.

In the enthusiasm to force the Eocene-Oligocene extinctions into the mold of the Cretaceous-Tertiary impact hypothesis and the periodic extinction hypothesis (Raup & Sepkoski 1984), a lot of misinformation has appeared. Typically, impact proponents treat the Eocene-Oligocene tran-